Research Square

Preprints are preliminary reports that have not undergone peer review.
They should not be considered conclusive, used to inform clinical practice,
or referenced by the media as validated information.

Nf2 inactivation in Foxj1-ependymal cells induces early ependymal tumorigenesis in the mouse

Pauline Marijon

pauline.marijon@aphp.fr

Pitié-Salpêtrière Hospital

Tuan Le Van

Sorbonne Université, Groupe Hospitalier Pitié-Salpêtrière

Antoine Blouin

Sorbonne Université, Groupe Hospitalier Pitié-Salpêtrière

Franck Bielle

Pitié-Salpêtrière Hospital

Julien Boetto

Sorbonne Université, Groupe Hospitalier Pitié-Salpêtrière

Matthieu Peyre

Pitié-Salpêtrière Hospital

Fausto Rodriguez

UCLA Health

Michel Kalamarides

Pitié-Salpêtrière Hospital

Research Article

Keywords:

Posted Date: November 13th, 2026

DOI: https://doi.org/10.21203/rs.3.rs-11525128/v1

License: This work is licensed under a Creative Commons Attribution 4.0 International License.
Read Full License

Additional Declarations: No competing interests reported.

Nf2 inactivation in *Foxj1*-ependymal cells induces early ependymal tumorigenesis in the mouse

Marijon P.[1,2], Le Van T.[1,2], Blouin A[1,2], Bielle F.[3], Boetto J.[1,2], Peyre M.[1,2], Rodriguez F.[4], Kalamarides M.[1,2]

[1] Sorbonne Université - Department of Neurosurgery, Bâtiment Babinski, Groupe Hospitalier Pitié-Salpêtrière, APHP, 47-83 boulevard de l'Hôpital, 75013, Paris, France.
[2] Neurovascular interfaces in Brain Tumors and Vascular Malformations -CRICM INSERM U1127 CNRS UMR 7225 – Paris Brain Institute, Hôpital de la Pitié-Salpêtrière, Paris, France.
[3] Sorbonne Université - Department of Neuropathology, Bâtiment Babinski, Groupe Hospitalier Pitié-Salpêtrière, APHP, 47-83 boulevard de l'Hôpital, 75013, Paris, France.
[4] UCLA Health – Department of Pathology and Laboratory Medicine, 10833 Le Conte Ave, 18-170 NPI Los Angeles, CA 90095-1732

Corresponding author: Marijon Pauline (pauline.marijon@aphp.fr)

ABSTRACT

Purpose: Spinal ependymomas (SE) are the most frequent primary spinal tumor, harboring *NF2* mutations in most cases and characterized by development of solid and/or cystic masses and peritumoral edema associated with morbidity. To explore the developmental and cellular mechanisms underlying these lesions and establish a reliable preclinical model, we generated a mouse model with *Nf2* inactivation in *Foxj*1-expressing ependymal cells, after confirming FOXJ1 expression in SE cells.

Methods: *FoxJ1Cre*^{ERT};*Nf2*$^{flox/flox}$ mice were generated, *Nf2* inactivation was induced at different developmental stages of high FoxJ1 expression (E16, P0–4, P15) using a tamoxifen-inducible system. Mice were monitored for up to 15 months, with extensive histopathological analysis and post-mortem MRI in selected cases. Multiplex immunofluorescence was performed to characterize proliferative ependymal regions and identify potential progenitor-like populations.

Results: Conditional *Nf2* inactivation resulted in frequent ependymal proliferations (87%) and cystic dilations of the central canal (54%), mimicking human pathological features. These spinal proliferations were often associated with intracranial hydrocephalus and periventricular lesions, particularly after P15 induction. Early induction (E16, P0–P4) caused higher mortality and malformations, whereas the P15 cohort showed a reproducible phenotype with minimal lethality. No frank tumor formation was detected in any cohort. Human SE and mouse proliferative lesions shared FoxJ1^{+} ependymal cells and FoxO3^{+}/GFAP^{+}/S100β^{-} populations resembling immature radial glial-like progenitors.

Conclusion: *Nf2* loss in differentiated ependymal cells induces frequently proliferation and cystic dilation of the central canal, characterizing early tumorigenic changes of SE. This mouse model provides a valuable preclinical platform for studying the earliest stages of SE pathogenesis and testing new therapeutic approaches.

INTRODUCTION

Spinal ependymomas (SE) account for approximately 10% of all central nervous system ependymomas and represent the most frequent glial tumors of the spinal cord (1). They differ markedly from other ependymoma subtypes in both localization and tumorigenic mechanisms, which are often driven by specific gene fusions and molecular signatures (2). Among the ten molecularly defined ependymoma subgroups, SE are uniquely characterized by biallelic inactivation of the *NF2* tumor suppressor gene identified in more than 90% of cases, whether they occur sporadically or in the context of *NF2*-related Schwannomatosis (*NF2*-SWN), underscoring the central role of the *NF2* gene in regulating ependymal cell proliferation. The most frequent tumor locations are cervical and cervicothoracic, and in approximately 75% of cases, the lesion includes a solid nodule associated with cystic components (3). They are typically diagnosed only after the onset of neurological symptoms, leading to early surgical management which remains the gold standard, balancing oncological control and functional preservation (4).

While human SE show biallelic *NF2* inactivation, their cell of origin and early developmental mechanisms remain poorly understood. Experimental studies in mice have suggested that mature ependymal cells, although traditionally considered terminally differentiated, retain latent plasticity and can re-enter the cell cycle under specific conditions such as injury or gene disruption (5). This capacity may be influenced by the *Nf2* tumor suppressor, which regulates cell–cell adhesion and contact-dependent growth arrest during tissue morphogenesis (6).
Herein, we used the *FOXJ1* gene, a specific marker of human SE and ependymal cells.in the mouse (5,7). We leveraged this marker to target *Nf2* inactivation in *Foxj1*-expressing cells at different time points using a tamoxifen -inducible model allowing specific temporal control of *Nf2* deletion. We observed early ependymal tumorigenesis and we also investigated the nature of the progenitor cells of the SE and we showed that SE and mouse ependymal proliferations shared a similar phenotype with persistence of immature precursor cell populations.

MATERIAL AND METHODS

Histology and immune-histochemistry of human SE

Human SE slides were reviewed to confirm the diagnosis. FOXJ1 immuno-histochemistry was performed (Merck, HPA005714, 1/500). Immature cells were assessed with GFAP (Abcam, ab7260, 1/1000), FOXO3 (Fisher, 16817513, 1/500), BLBP (Abcam, ab32423, 1/100), S100β

(Sigma Aldrich, ABN59, 1/500), OLIG2 (Sigma Aldrich, AB9610, 1/1000). Multiplex staining was done with Opal technology (Akoya Biosciences, USA), and automated cells quantification applied after calibration on fluorescence.

Generation of the *FoxJ1Cre$^{ERT/WT}$;Nf2$^{flox/flox}$* mice

Foxj1Cre$^{ERT2:GFP/WT}$ mice (Jackson Laboratory®) (8) were double-crossed with *Nf2$^{flox/flox}$* mice to generate *FoxJ1Cre$^{ERT/WT}$;Nf2$^{flox/flox}$* progeny. Cre recombination was induced by tamoxifen administration at distinct developmental stages to capture the peak periods of *Foxj1* expression (5). Genotyping was performed using tail biopsies collected from each mouse during the first week of life. RNA was extracted from these samples, allowing determination of the genotype of each animal and subsequent allocation to the appropriate experimental cohorts. Tail biopsies were performed using an established and appropriate procedure, within the recommended time frame, to ensure animal welfare.

Tamoxifen induction protocols

Three cohorts were established according to already published Foxj1 expression peaks: prenatal (E16), early postnatal (P0–P4), and late postnatal (P15) (5). Appropriate controls were included (corn oil–injected *FoxJ1Cre$^{ERT/WT}$;Nf2$^{flox/flox}$* mice and *FoxJ1Cre$^{ERT/WT}$;Nf2$^{WT/WT}$* with tamoxifen injection). Tamoxifen was delivered by oral gavage of pregnant females (E16, 0.05mg/g.), intraperitoneal injection in lactating females (P0–P4, 0.075mg/g, one intraperitoneal injection per day to the dam for four consecutive days), or intraperitoneal injection (P15 mice, 0.1mg/g).

Monitoring and tissue processing

Mice were observed for up to 15 months and sacrificed at endpoint or upon neurological signs. Brain and spinal cord were removed as a single piece using retrograde hydraulic extrusion, preserving anatomical continuity for histology. After euthanasia, the skull was opened using scissors, and the brain was carefully dissected by severing the cranial nerves while keeping the brain connected to the spinal cord. The vertebral column was then transected just above the base of the tail to expose the vertebral canal. A 20G cannula was inserted into the spinal canal, and cold sterile water was injected under controlled pressure (a volume of 1 mL was injected over 1–2 seconds). This hydraulic pressure enabled the ejection of the entire CNS—brain and spinal cord—as an intact unit through the cranial cavity. This technique minimizes mechanical damage and preserves the anatomical continuity of the CNS for downstream analyses (Supplementary Fig 1).

At six months post-induction, three *FoxJ1Cre*$^{ERT/WT}$;*Nf2*$^{flox/flox}$ mice from the P15 cohort were sacrificed for interim analysis. The spinal cord and brain were collected and processed as described above to assess early histopathological changes before the onset of overt cystic lesions or ependymal disorganization. This intermediate timepoint was chosen to evaluate whether *Nf2* inactivation in ependymal cells led to progressive rather than immediate abnormalities.

Spinal cords (axial) and brains (coronal) were serially sectioned every 400 µm, generating two consecutive sections at each level; every other section was stained with HE. A selected set of slides was reassessed by an expert neuropathologist (F. R.).

In addition to paraffin-embedded specimens, a subset of spinal cords and brains, was freshly dissected and rapidly frozen in isopentane cooled by liquid nitrogen. Cryostat sections (5 µm) were prepared and fixed in 4% paraformaldehyde for 10 min before immunostaining. FoxJ1 immunofluorescence was performed on these frozen sections to validate antigen preservation and to visualize ependymal cell organization under conditions minimizing fixation-related artifacts.

MRI acquisition

Post-mortem spinal MRI was performed on an 11.7 Tesla Bruker BioSpec MRI with optimized T1/T2 protocols (ParaVision 360 software) and 38mm volume coil. Mice were euthanized immediately before scanning to prevent motion artifacts. Imaging enabled clinico-radiological correlation with observed phenotypes. MRI Imaging required a 4-hour acquisition time per mouse.

Immunohistochemistry and multiplex immunofluorescence of mouse tissues

Foxj1 immunohistochemistry was performed on frozen spinal cord sections. Multiplex immunofluorescence (Foxj1, Gfap, Foxo3, Blbp, S100β, Olig2, the same antibodies as described in the section above were used.) were performed on selected sections showing ependymal proliferation. Multiplex staining was performed using Opal™ technology (Akoya Biosciences, Marlborough, MA, USA). Slides were scanned and analyzed with automated fluorescence quantification software after calibration.

RESULTS

FOXJ1 is expressed in human spinal ependymomas

To confirm a previous work (9) that showed that low-grade ependymoma share a FOXJ1 ciliogenesis program with their normal tissue counterparts, we analyzed 16 paraffin-embedded tissue blocks from patients operated on for *NF2*-SWN or sporadic SE demonstrating strong nuclear FOXJ1 positivity (16/16, 100%) within tumor cells (Fig 1), without difference between *NF2*-SWN and sporadic. This finding confirms the ependymal differentiation of the neoplastic cells and reflects preservation of their functional ciliogenic program (10).

Generation of a mouse model and identification of the best timing for *Nf2* biallelic inactivation in *Foxj1*-expressing ependymal cells

The consistent and strong expression of FOXJ1 in SE supports its value as a reliable marker of ependymal lineage to target biallelic*Nf2* inactivation. To determine whether $FoxJ1Cre^{ERT/WT}$ mediated *Nf2* inactivation results in ependymoma formation, we generated 3 cohorts of $FoxJ1Cre^{ERT/WT};Nf2^{flox/flox}$ mice with injection of Tamoxifen at 3 different timepoints representing the physiological peaks of Foxj1 expression in mice (5).

The late postnatal cohort (tamoxifen at P15) was the easiest to generate, with the lowest mortality rate. It included 24 experimental mice and 10 control mice. Three additional mice were euthanized after 6 months of follow-up for an early histological analysis, none of which exhibited clinical manifestations. At 15 months, 12 exhibited a generalized reduction in motor activity, and one animal showed clinical features consistent with epileptic seizures. In contrast, no clinical abnormalities were observed in the control mice. The prenatal cohort (tamoxifen at E16) included 17 experimental mice and 6 controls. This cohort was more difficult to generate, as gavage of pregnant females resulted in a high number of miscarriages (40-50%). The early postnatal cohort (tamoxifen at P0P4) consisted of 15 experimental mice and 2 controls. This group was particularly challenging to generate due to high pup mortality during the first weeks of life.

***Foxj1* -directed biallelic *Nf2* inactivation leads to the development of ependymal cell proliferation and cyst dilatation.**

Histological analysis performed on mice euthanized at 6 months (P15) showed an ependymal proliferation associated with cystic dilatation of the ependymal canal in 2 out of 3 animals. After 15 months, histological analysis of spinal cords showed a phenotype predominantly in the cervical portion of the spinal cord (Fig.1C). Ependymal cell proliferation defined by the presence of more than two layers of ependymal cells around the ependymal canal was observed in most cases (n=21, 87%) (Fig.1D-E), frequently associated with a cystic dilation of the

ependymal canal (n=13, 54%) (Fig.1F-G). Hydrocephalus and periventricular proliferations were observed in 83% and 12% of cases respectively.
The mouse with epileptic seizures showed no additional cerebral lesions beyond hydrocephalus, a feature also observed in other mice.

For the prenatal cohort (tamoxifen at E16), after 15 months, histological analysis of spinal cords showed cystic dilation of the ependymal canal (n=8, 47%), along with ependymal cell proliferation (n=14, 82%). Hydrocephalus and periventricular proliferations were observed in 53% of cases.
For the early post-natal cohort (tamoxifen at P0P4), histological analysis did not reveal proliferative or cystic lesions; instead, only malformations and structural anomalies were observed.
No tumor formation, particularly, SE was identified in any of the three cohorts.

We observed that the occurrence of ependymal cysts progressively decreased from the cervical to the lumbar region, consistent with a gradient in the severity of the ventricular wall alteration (Fig. 2A). Cervical segments most frequently exhibited two ependymal layers or overt ependymal proliferation, whereas thoracic segments showed fewer and milder alterations. In contrast, lumbar regions displayed an intermediate phenotype, with fewer two-layered structures but a re-emergence of proliferative changes in some specimens (Fig. 2B). The heatmap in Figure 2C illustrates the heterogeneity of these phenotypes at the individual-mouse level, highlighting that although the cervical region consistently presents the highest pathological scores, the thoracic and lumbar segments display variable combinations of two-layering, proliferation, and cyst formation. Together, these observations indicate a region-dependent vulnerability of the ependymal lining, with the cervical spinal cord being the most susceptible to structural and proliferative abnormalities. These analyzes were performed in P15 subgroup.
Post-mortem MRI performed in three P15-mice revealed cystic dilatations of the ependymal canal at the cervicothoracic level in 2 out of 3 animals. Subsequent histological analysis of these spinal cords confirmed the presence of these cystic dilatations at the same location identified by MRI (Fig. 3).

Investigation of radial glial cell populations in human SE and mouse model

To further characterize the tumoral cells, we performed multiplex immunofluorescence analyses on a cohort of human *NF2*-SWN (n = 16) and sporadic SE (n = 8) showing the presence of radial glial-like progenitor populations within SE. Tumoral cells co-expressing GFAP and FOXO3 were identified, together with a subset of $GFAP^{+}/FOXO3^{+}/BLBP^{+}$ cells lacking expression of S100β, OLIG2, and FOXJ1, supporting the presence of immature, progenitor-like populations within these tumors.

We then sought to determine whether this type of cell was found in ependymal proliferations in our mouse model. In $FoxJ1Cre^{ERT/WT};Nf2^{flox/flox}$, we first detected strong Foxj1 staining in all ependymal proliferations assay that were test (n = 8) (Fig. 4A). We identified a population of $Foxo3^{+}/Gfap^{+}/S100\beta^{-}$ cells within the ependymal proliferations (Fig. 4B), characterized by nuclear *Foxo3* expression and astroglial lineage commitment ($Gfap^{+}$) while lacking the mature ependymal marker S100β. This immunophenotypic profile is consistent with the presence of radial glial-like progenitor cells and suggests the persistence of immature precursor populations within the lesions. The recapitulation of the cellular phenotype observed in human SE further supports the relevance of this mouse model for studying the early stages of *Nf2*-driven SE development.

DISCUSSION

This study provides the first comprehensive characterization of a conditional $FoxJ1Cre^{ERT/WT};Nf2^{flox/flox}$ mouse model reproducing the earliest pathological stages of *Nf2*-associated SE development. *Nf2* biallelic inactivation in *FoxJ1*-expressing cells induced very often focal ependymal proliferations and cystic dilations of the central canal of the spinal cord recapitulating hallmark features of human *NF2*-associated SE, predominantly at the cervical location This suggests that *Nf2* bi-allelic inactivation induced “ependymal proliferations,” microscopic lesions that represent early stages of ependymal tumorigenesis. Similar observations have been reported in *Nf2*-deficient mouse models of meningioma and schwannoma, in which loss of *Nf2* is sufficient to trigger focal hyperplastic or pre-neoplastic lesions (11,12). In meningeal tissues, *Nf2* inactivation results in proliferative arachnoidal lesions that resemble early meningioma formation, whereas in Schwann cells it promotes Schwann cell hyperplasia and precursor lesions preceding schwannoma development. (11,12). Frequent proliferative alterations (87%) and cystic canal dilations (54%) confirmed by

immediate post-mortem MRI, represent a pre-tumoral state. Notably, ependymal hyperplasia proliferation was already detectable in animals examined at 6 months of age, suggesting that these lesions arise relatively early in life and may represent an early consequence of *Nf2* inactivation. We hadn't designed the protocol for an early study of tumorigenesis, but clearly, that still needs to be done to determine at what point this mouse model exhibits a usable phenotype. A previous study in mice have demonstrated that *Nf2* regulates cell–cell adhesion during tissue fusion and that Nf2 protein is required to stabilize the junctional complex (tight and adherent junctions) (6). In absence of merlin, the ependymal cells cannot form junctions and are unable to form a well-organized tissue and are resistant to contact-dependent growth arrest, producing multilayers, a first step of tumorigenesis as observed in our mouse model.

Clinically, spinal ependymomas predominate in the cervical and cervico-thoracic spinal cord (3,13,14), mirroring our finding that the cervical segment shows the most pronounced ependymal two-layering and proliferative changes. Given its consistent and severe involvement, the cervical cord represents the most tractable region for analysis, restricting studies to a well-defined, reproducible compartment. Ependymal hyperplasia was already detectable by 6 months of age, indicating relatively early onset; whether still earlier lesions exist remains to be tested. Overall, these findings support the $FoxJ1Cre^{ERT/WT};Nf2^{flox/flox}$ mouse model as a practical, reproducible preclinical platform for studying early *Nf2*-driven ependymal alterations, with tamoxifen induction at P15 offering the best balance between phenotype penetrance and survival compared with the E16 and P0–P4 groups and cervical spinal cord analysis being

The question of the ependymoma cell of origin remains debated. In SE, molecular and transcriptomic data point to a derivation from radial glial-like or ependymal progenitors of the central canal, rather than from the multipotent neuroepithelial stem cells implicated in supratentorial subtypes (15). Although post-mitotic under physiological conditions, ependymal cells retain latent plasticity; after spinal cord injury, $Foxj1^{+}$ ependymal cells dedifferentiate, migrate to the lesion site, and redifferentiate into astrocytic or oligodendroglial lineages, contributing to tissue repair (16–18), a cellular response closely paralleled in ependymoma models.

Consistent with this hypothesis, our multiplex immunofluorescence identified in human SE immature glial-like cells co-expressing GFAP and FoxO3 but lacking the mature astrocytic marker S100β, with variable BLBP expression and heterogeneous Olig2/FoxJ1 status. While

this heterogeneity, also reported in RNA-seq studies (19), does not permit definitive identification of the cell of origin, it supports the persistence of progenitor-like states within *NF2*-SWN lesions, reminiscent of the transient radial glia identity present during embryonic. On the mouse model generated in this study,s asimilar phenotype was observed in the ependymal proliferations with the presence of radial glial-like progenitor cells.

Our results suggesting the persistence of immature precursor populations within the lesions, are very preliminary but novel and need to be further investigated and confirmed, particularly through RNA-seq and multi-omics studies in humans and mice.

CONCLUSION

In summary, this conditional *FoxJ1Cre*$^{ERT/WT}$/*Nf2*$^{flox/flox}$ mouse model recapitulates the earliest stages of *Nf2*-driven SE pathogenesis, highlighting the roles of ependymal progenitor plasticity. It bridges developmental biology and clinical neuro-oncology, providing a robust framework for exploring both the mechanisms of tumor development and cystic progression and the efficacy of novel targeted therapies.

DECLARATIONS

Funding

This work was supported by a grant from NF2 BioSolutions.

Competing Interests

The authors have no relevant financial or non-financial interests to disclose.

Author Contributions

All authors contributed to the study conception and design. Material preparation, data collection and analysis were performed by Pauline Marijon. Tuan Le Van, Antoine Blouin and Julien Boetto performed material preparation. Franck Bielle and Fausto J. Rodriguez performed the neuropathological review and the interpretation of the histological analyses. Immunofluorescence analyses were performed by Pauline Marijon.

Matthieu Peyre and Michel Kalamarides supervised the project. The first draft of the manuscript was written by Pauline Marijon, and all authors commented on previous versions of the manuscript. All authors read and approved the final manuscript.

Ethics Approval

All animal procedures were performed in accordance with European Directive 2010/63/EU and French regulations, and the project was approved by the French Ministry of Higher Education and Research (APAFIS P188R, Accepted in 2020). Human spinal ependymoma samples were obtained from a declared biobank (Onconeurotek, ONT) in accordance with the Declaration of Helsinki and French regulations.

Consent to Participate

Patients were informed of the research use of their samples and did not object (non-opposition procedure), in accordance with French regulations.

Consent to Publish

Not applicable. No identifiable patient data are presented.

Data Availability

The datasets generated and analyzed during the current study are available from the corresponding author on reasonable request.

Acknowledgments

We thank the PHENO-ICMice core facility and Histomics for their technical support. This work was supported by a grant from NF2 BioSolutions.

References

1. Villano JL, Parker CK, Dolecek TA. Descriptive epidemiology of ependymal tumours in the United States. Br J Cancer. 2013 Jun 11;108(11):2367–71. doi:10.1038/bjc.2013.221 PubMed PMID: 23660944; PubMed Central PMCID: PMC3681017.
2. Pajtler KW, Witt H, Sill M, Jones DTW, Hovestadt V, Kratochwil F, et al. Molecular Classification of Ependymal Tumors across All CNS Compartments, Histopathological Grades, and Age Groups. Cancer Cell. 2015 May 11;27(5):728–43. doi:10.1016/j.ccell.2015.04.002 PubMed PMID: 25965575; PubMed Central PMCID: PMC4712639.
3. Aghakhani N, Messerer M, David P, Herbrecht A, Parker F. [Intramedullary ependymomas: A French retrospective multicenter study of 221 cases]. Neurochirurgie. 2017 Nov;63(5):391–7. doi:10.1016/j.neuchi.2016.07.002 PubMed PMID: 28162253.
4. Plotkin SR, O'Donnell CC, Curry WT, Bove CM, MacCollin M, Nunes FP. Spinal ependymomas in neurofibromatosis Type 2: a retrospective analysis of 55 patients. J Neurosurg Spine. 2011 Apr;14(4):543–7. doi:10.3171/2010.11.SPINE10350 PubMed PMID: 21294614.
5. Li X, Floriddia EM, Toskas K, Chalfouh C, Honore A, Aumont A, et al. FoxJ1 regulates spinal cord development and is required for the maintenance of spinal cord stem cell potential. Exp Cell Res. 2018 Jul 1;368(1):84–100. doi:10.1016/j.yexcr.2018.04.017 PubMed PMID: 29689278.
6. McLaughlin ME, Kruger GM, Slocum KL, Crowley D, Michaud NA, Huang J, et al. The Nf2 tumor suppressor regulates cell-cell adhesion during tissue fusion. Proc Natl Acad Sci U S A. 2007 Feb 27;104(9):3261–6. doi:10.1073/pnas.0700044104 PubMed PMID: 17360635; PubMed Central PMCID: PMC1801999.
7. Abedalthagafi MS, Wu MP, Merrill PH, Du Z, Woo T, Sheu SH, et al. Decreased FOXJ1 expression and its ciliogenesis programme in aggressive ependymoma and choroid plexus tumours. J Pathol. 2016 Mar;238(4):584–97. doi:10.1002/path.4682 PubMed PMID: 26690880; PubMed Central PMCID: PMC5364032.
8. Muthusamy N, Vijayakumar A, Cheng G, Ghashghaei HT. A knock-in Foxj1CreERT2::GFP mouse for recombination in epithelial cells with motile cilia. Genes N Y N 2000. 2014 Apr;52(4):350–8. doi:10.1002/dvg.22753 PubMed PMID: 24550157; PubMed Central PMCID: PMC3991760.
9. Marijon P, Teranishi Y, Bielle F, Sanson M, Peyre M, Kalamarides M. Comprehensive characterization of spinal ependymomas in NF2-Schwannomatosis. Acta Neuropathol Commun. 2026 May 28. doi:10.1186/s40478-026-02331-w PubMed PMID: 42210322.
10. Mukherjee I, Roy S, Chakrabarti S. Identification of Important Effector Proteins in the FOXJ1 Transcriptional Network Associated With Ciliogenesis and Ciliary Function. Front Genet. 2019 Mar 1;10:23. doi:10.3389/fgene.2019.00023 PubMed PMID: 30881373; PubMed Central PMCID: PMC6405523.
11. Kalamarides M, Niwa-Kawakita M, Leblois H, Abramowski V, Perricaudet M, Janin A, et al. Nf2 gene inactivation in arachnoidal cells is rate-limiting for meningioma development in the mouse. Genes Dev. 2002 May 1;16(9):1060–5. doi:10.1101/gad.226302 PubMed PMID: 12000789; PubMed Central PMCID: PMC186259.
12. Giovannini M, Robanus-Maandag E, van der Valk M, Niwa-Kawakita M, Abramowski V, Goutebroze L, et al. Conditional biallelic Nf2 mutation in the mouse promotes manifestations of human neurofibromatosis type 2. Genes Dev. 2000 Jul 1;14(13):1617–30. PubMed PMID: 10887156; PubMed Central PMCID: PMC316733.
13. Benesch M, Frappaz D, Massimino M. Spinal cord ependymomas in children and adolescents. Childs Nerv Syst ChNS Off J Int Soc Pediatr Neurosurg. 2012 Dec;28(12):2017–28. doi:10.1007/s00381-012-1908-4 PubMed PMID: 22961356.

14. Kalamarides M, Essayed W, Lejeune JP, Aboukais R, Sterkers O, Bernardeschi D, et al. Spinal ependymomas in NF2: a surgical disease? J Neurooncol. 2018 Feb;136(3):605–11. doi:10.1007/s11060-017-2690-7 PubMed PMID: 29188529.
15. Taylor MD, Poppleton H, Fuller C, Su X, Liu Y, Jensen P, et al. Radial glia cells are candidate stem cells of ependymoma. Cancer Cell. 2005 Oct;8(4):323–35. doi:10.1016/j.ccr.2005.09.001 PubMed PMID: 16226707.
16. Meletis K, Barnabé-Heider F, Carlén M, Evergren E, Tomilin N, Shupliakov O, et al. Spinal cord injury reveals multilineage differentiation of ependymal cells. PLoS Biol. 2008 Jul 22;6(7):e182. doi:10.1371/journal.pbio.0060182 PubMed PMID: 18651793; PubMed Central PMCID: PMC2475541.
17. Sabelström H, Stenudd M, Réu P, Dias DO, Elfineh M, Zdunek S, et al. Resident neural stem cells restrict tissue damage and neuronal loss after spinal cord injury in mice. Science. 2013 Nov 1;342(6158):637–40. doi:10.1126/science.1242576 PubMed PMID: 24179227.
18. Barnabé-Heider F, Göritz C, Sabelström H, Takebayashi H, Pfrieger FW, Meletis K, et al. Origin of new glial cells in intact and injured adult spinal cord. Cell Stem Cell. 2010 Oct 8;7(4):470–82. doi:10.1016/j.stem.2010.07.014 PubMed PMID: 20887953.
19. Garcia C, Gutmann DH. Nf2/Merlin Controls Spinal Cord Neural Progenitor Function in a Rac1/ErbB2-Dependent Manner. PLoS ONE. 2014 May 9;9(5):e97320. doi:10.1371/journal.pone.0097320 PubMed PMID: 24817309; PubMed Central PMCID: PMC4016309.

Figure

Figure 1

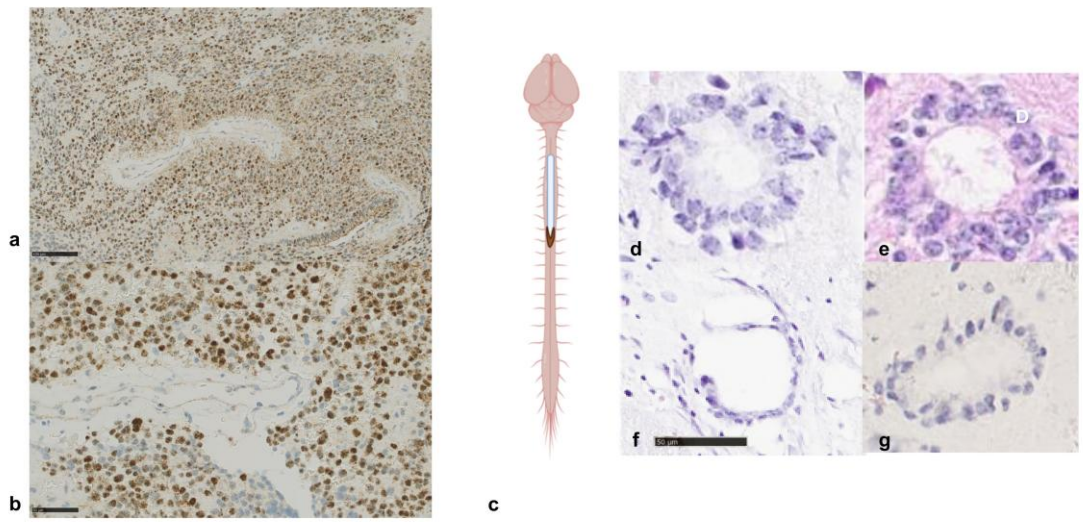


Figure 1: *Overview of histological findings in FoxJ1$^{Cre/WT}$/Nf2$^{flox/flox}$ mice*

A and B : FoxJ1 (DAB) in human ependymoma. C: Schematic representation of abnormalities found during histological analysis. D: Two ependymal layers, at P15, cervical axial section. E: Ependymal multilayer, at P15, cervical axial section. F: Cystic dilatation of ependymal canal

with flattening of ependymal cells, at P15, cervical axial section. G: Ependymal canal without anomalies, at P15, cervical section.

Figure 2

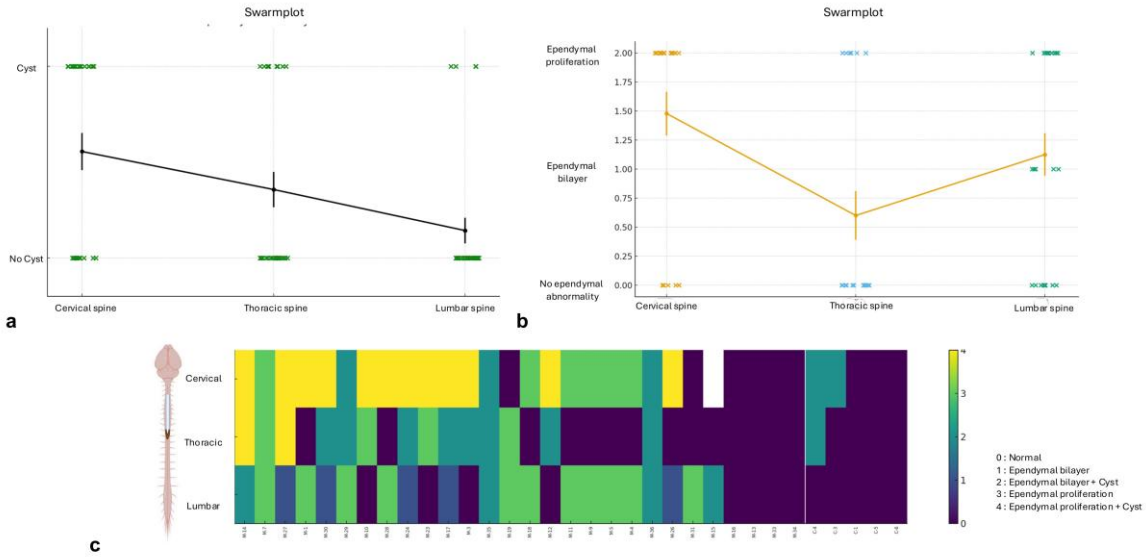
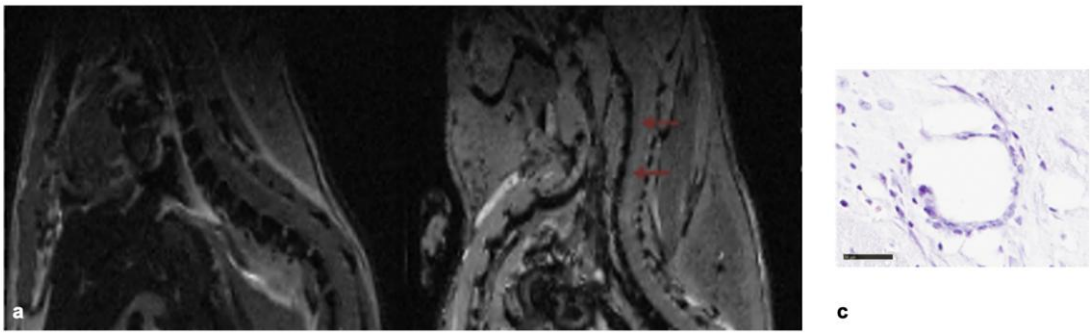


Figure 2: *Regional distribution of ependymal abnormalities along the spinal axis in the Nf2-mutant mouse model.*

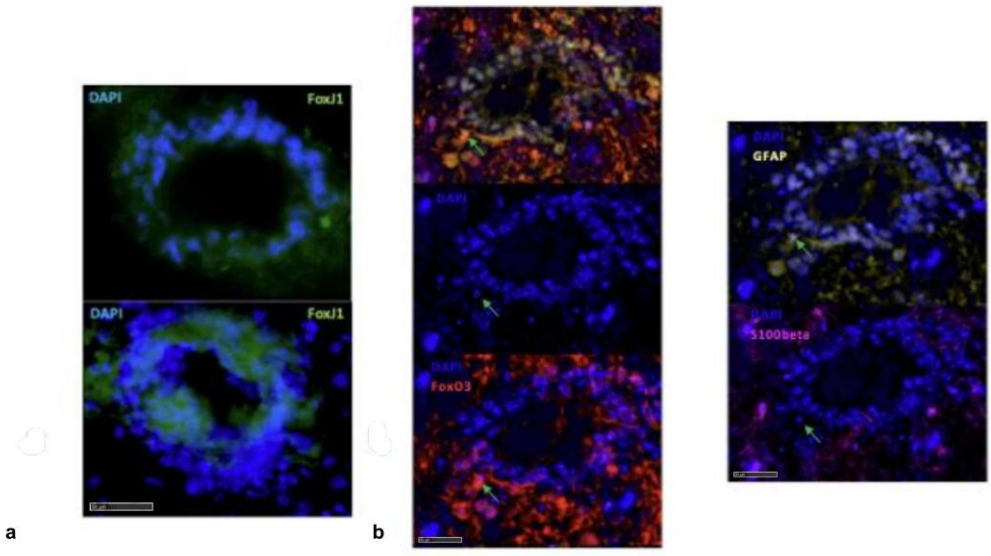
A: Incidence of ependymal cysts across cervical, thoracic, and lumbar spinal levels. Individual data points represent animals, and the line indicates the mean ± SEM. B: Distribution of ependymal dysplasia scored as: no abnormality, ependymal two-layer, or ependymal proliferation. Individual values and mean ± SEM are shown. C: Heatmap summarizing the combined severity of ependymal abnormalities and cyst formation in each spinal segment for all mice analyzed. Color codes correspond to: 0 = normal; 1 = ependymal bilayer; 2 = ependymal bilayer + cyst; 3 = ependymal proliferation; 4 = ependymal proliferation + cyst. The anatomical diagram on the left indicates the rostro–caudal orientation of the spinal cord. The animals labeled ‘C’ on the right side of the heatmap correspond to control mice.

Figure 3



418
419
420 **Figure 3:** *Post-mortem mouse spine MRI*
421 A: Axial T1- and T2-weighted MRI sequences of the spinal cord from a P15 mouse, showing
422 dilation of the ependymal canal (red arrows). B: Axial section of the cervical spinal cord at the
423 level corresponding to the MRI images shown above.

Figure 4



424

Figure 4: *Immunofluorescence in spine of FoxJ1$^{Cre/WT}$/Nf2$^{flox/flox}$ mice*

A: Immunofluorescent staining for FOXJ1 highlighting intense expression within a periependymal proliferative area in a P15 mouse. B: Multiplex immunofluorescence staining (GFAP, FoxO3, S100β) identifying a GFAP-positive, FOXO3-positive, S100β-negative (green arrow) cell at the margin of the ependymal canal in a P15 mouse.

Supplementary Figure 1: *One piece extraction of the mouse central nervous system.*

A: One piece extraction of a mice CNS. B: Step of one-piece (en bloc) extraction of the mouse central nervous system

Supplementary Files

This is a list of supplementary files associated with this preprint. Click to download.

- Fig1sup.tif